Biogeosciences Discuss., 10, 16903–16922, 2013
www.biogeosciences-discuss.net/10/16903/2013/
doi:10.5194/bgd-10-16903-2013

Biogeosciences Discussions
Open Access

On the stratigraphic integrity of leaf-wax biomarkers in loess-paleosols

C. Häggi, R. Zech, C. McIntyre, and T. Eglinton

Geological Institute, ETH Zurich, Switzerland

Received: 30 September 2013 – Accepted: 16 October 2013 – Published: 29 October 2013

Correspondence to: R. Zech (zech@erdw.ethz.ch)

Published by Copernicus Publications on behalf of the European Geosciences Union.

Abstract

Paleoenvironmental and paleoclimate reconstructions based on molecular proxies, such as those derived from leaf wax biomarkers, in loess-paleosols sequences represent a promising line of investigation in Quaternary research. The main premise of such reconstructions is the synsedimentary deposition of biomarkers and dust, which has become a debated subject in recent years. This study uses two independent approaches to test the stratigraphic integrity of leaf-wax biomarkers: (i) Long-chain *n*-alkanes and fatty acids are quantified in two soil profiles in till on the Swiss Plateau. Since glacial sediments are extremely poor in organic matter, significant amounts of leaf-wax biomarkers in the lower part of those profiles would reflect post-sedimentary root-derived or microbial contributions. (ii) Compound-specific radiocarbon measurements are conducted on *n*-alkanes and fatty acids from several depth intervals in the loess section "Crvenka", Serbia, and the results are compared to independent estimates of sediment age. We find extremely low concentrations of plant wax *n*-alkanes and fatty acids below the topsoils in the soil profiles. Moreover, compound-specific radiocarbon analysis yields plant wax ^{14}C ages that agree well with published luminescence ages and stratigraphy of the Serbian loess deposit. Both approaches confirm that post-sedimentary, root-derived or microbial contributions are negligible in the two systems investigated. The good agreement between *n*-alkane and fatty acid ages, as well as between odd and even homologues, further indicates that reworking and incorporation of fossil leaf-waxes is not particularly relevant either.

1 Introduction

Biomarkers or chemical fossils are relatively poorly decomposable components of plants, microorganisms and animals, which, in some cases, record past environmental conditions (Eglinton and Eglinton, 2008). Over the last decade, biomarker analyses in loess-paleosol sequences (LPS) have become an increasingly important tool for pa-

BGD
10, 16903–16922, 2013

leoclimate reconstructions. The distributions of plant-waxes, particularly long-chain *n*-alkanes and fatty acids, are used to reconstruct past vegetation (Xie et al., 2002; Zhang et al., 2006; Zech et al., 2010; Zech et al., 2009b), while stable carbon isotopic ($\delta^{13}C$) and D/H analyses of these compounds provide valuable information about changes in paleohydrology and paleoclimate (Liu and Huang, 2005; Zech et al., 2011b, 2013).

The main premise of such reconstructions is the assumption that the biomarkers are deposited synsedimentary with dust and are not subject to significant overprinting. For long-chain *n*-alkanes and fatty acids, which are thought to be mainly produced above ground as epicuticular leaf-waxes, this assumption seems reasonable given their low solubility and hence limited mobility. However, pre-aged organic matter can be transported by wind and re-deposited together with dust (Liu et al., 2007; Eglinton et al., 2002). Moreover, Gocke et al. (2010, 2013) suggested that significant amounts of long-chain *n*-alkanes and fatty acids are produced within rhizoliths in the vicinity of root systems. Labeling experiments have also suggested potentially significant contributions of root-derived plant-wax biomarkers (Wiesenberg et al., 2010). Furthermore, litter bag studies indicate some microbial production of long-chain *n*-alkanes in the early stages of litter degradation (Nguyen Tu et al., 2011; Zech et al., 2011a). Each of these processes could potentially overprint the original biomarker signal laid down at the time of deposition. The quantification of the above effects and their implications for plant wax lipid-based proxy reconstructions remains equivocal.

In the present study two different approaches were chosen to evaluate the stratigraphic integrity of leaf-wax biomarkers:

(i) Two soil profiles in till on the Swiss Plateau were analyzed for their biomarker concentrations. As glacial sediments are extremely poor in organic material, the presence of significant amounts of leaf-wax markers would indicate post-sedimentary contributions from roots and/or microorganisms.

(ii) Compound-specific radiocarbon analysis was performed on leaf-waxes extracted from selected intervals from a LPS in Serbia and compared to independent, pub-

BGD
10, 16903–16922, 2013

lished ages for this section based on luminescence and stratigraphy, as well as bulk organic carbon ^{14}C ages.

2 Material and methods

2.1 Geographical setting and sampling

2.1.1 Soil profiles in till on the Swiss Plateau

Two soil profiles on the Swiss Plateau were sampled in summer 2012: An abandoned quarry near Niederbuchsiten (483 m a.s.l.; 47.286° N, 7.780° E), and a 2 m deep profile dug near Steinhof (593 m a.s.l.; 47.155° N, 7.682° E). The site near Niederbuchsiten comprises a luvisol developed in till, which is thought to have been deposited during the penultimate glaciation, i.e. before 130 ka (Bitterli et al., 2011). An A_h horizon at the top 30 cm of the profile overlies the B_t horizon, which is followed by the C horizon below 3 m depth. Seven samples were collected to a depth of ~ 6 m (Fig. 1a). The Steinhof site is situated close to the north-western edge of the last glacial maximum extent of the Valais Glacier, and the till there was likely deposited ~ 20 ka ago (Bini et al., 2009; Bitterli et al., 2011; Ivy-Ochs et al., 2004). The top 35 cm of the Steinhof profile are an A_h horizon, followed by a B_t horizon (35–200 cm depth). The decalcification depth was reached in a core at 3.9 m. Seven samples were collected approximately every 30 cm down to a depth of 2 m (Fig. 1b).

2.1.2 The loess-paleosol sequence Crvenka

The LPS Crvenka is situated in a brickyard on the southwestern edge of the Baĕka loess plateau, 150 km northwest of Belgrade, Serbia (45°39.750′ N, 19°28.774′ E, altitude 108 m a.s.l.). The profile consists of a Holocene-age topsoil that caps about 8 m of loess attributed to marine isotope stage (MIS) 2 and MIS 4 (Fig. 1c). A weakly developed paleosol complex formed during MIS 3 (i.e. between ~ 58 and 28 ka), and is

BGD
10, 16903–16922, 2013

found between 4–5.5 m. Below the MIS 4 loess, at ∼ 8 m depth, a well developed 2 m thick clay-rich paleosol follows, documenting intensive pedogenesis and reduced dust accumulation during MIS 5 (∼ 130 to 75 ka). The lowermost part of the section consists of loess deposited during MIS 6. Modern roots are found in the Holocene topsoil and the upper parts of the MIS 2 loess. Fossil roots are evident in the MIS 3 and MIS 5 paleosols and the upper parts of the underlying MIS 4 and MIS 6 loess units. Previous studies in the LPS Crvenka were conducted using a wide range of analytical tools, including magnetic susceptibility, grain size analysis, geochemistry, and biomarkers (Marković et al., 2008; Zech et al., 2009a; Zech et al., 2013). Extensive chronological work has also been conducted using optically stimulated luminescence (OSL) and elevated temperature post-IR infrared stimulated luminescence (post-IR IRSL) (Stevens et al., 2011).

For this study, four samples from a field campaign in summer 2009 were selected (Fig. 1c): One sample from the Holocene topsoil (25 cm depth, label: Cr 1), one from the MIS 2 loess (2 m depth, Cr 10), one from the MIS 3 paleosol (4 m depth, Cr 20), and one from the top of the MIS 5 paleosol (8 m depth, Cr 40). The depositional ages of these four samples are estimated based on stratigraphy and luminescence as Holocene (Cr 1), 23 ± 2 ka (Cr 10), 28 ± 2 ka (Cr 20), and > 75 ka (Cr 40). While the age of Cr 10 is well constrained with luminescence (Stevens et al., 2011), an age of 28 ka for Cr 20 represents an estimation. This age is constrained by luminescence ages of 22 ka and 33 ka above and below our sample, and represents the boundary age between the Middle and Upper Pleniglacial immediately following Greenland Interstadial 3 (Kadereit et al., 2013). Using this chronostratigraphic concept instead of the currently accepted MIS boundaries is justifiable for terrestrial records.

2.2 Sample preparation and analyses

The samples from the Swiss soil profiles were freeze-dried (Christ ALPHA LDplus), homogenized gently, and sieved to < 2 mm. The loess samples from Crvenka were dried at room temperature. Free lipids were obtained from sample aliquots (30–40 g dry

BGD
10, 16903–16922, 2013

weigth) with a Dionex ASE 200 accelerated solvent extractor using dichloromethane (DCM) and methanol (MeOH; 9 : 1) at 1500 psi and 100 °C. The total lipid extracts were separated over aminopropyl columns. *n*-Alkanes were eluted with hexane, more polar lipids eluted with DCM : MeOH (1 : 1), and free fatty acids were eluted with diethyl ether:acetic acid (19 : 1). The fatty acid fraction was methylated at 80 °C with methanolic HCl (MeOH δ^{14}C: −995.6 ‰): yielding the corresponding fatty acid methyl esters (FAMEs). The compounds were recovered by liquid–liquid extraction using hexane and were subsequently cleaned over silica columns. Fatty acid and *n*-alkane concentrations were determined using an Agilent Technologies 7890A gas chromatograph (GC) equipped with a VF1 column (30 m, 0.25 mm, 0.25 µm) and a flame ionization detector (FID). Compounds were quantified using 5α-androstane and identified by comparison with external standards.

The *n*-alkanes and FAMEs for compound-specific radiocarbon dating were further purified using $AgNO_3$ and zeolite (Geokleen) pipette columns. The zeolite, which occludes straight-chain (*n*-alkyl) compounds, was dissolved in HF after drying, and target compounds were then recovered by liquid–liquid extraction with hexane. Specific *n*-Alkane and FAME homologues were isolated using a Gerstel Preparative Fraction Collector coupled to an Agilent Technologies 7890A GC system equipped with a VF1 column (30 m, 0.53 mm, 0.5 µm). The isolated compounds were recovered with DCM, passed through pipette columns (SiO_2) to remove column bleed, and transferred to quartz tubes. After removal of solvent, a small quantity of CuO was added before the tubes were evacuated to 10^{-3} mbar over a vacuum line and flame sealed. Compounds were combusted at 850 °C for 6 h and the resulting CO_2 was purified over a ∼ −70 °C butylacetate water trap on a vacuum line. CO_2 was then quantified manometrically and subsequently sealed in Pyrex tubes. Radiocarbon measurements were conducted on the ETH Hönggerberg MICADAS AMS system (Synal et al., 2007; Wacker et al., 2013).

For total organic carbon (TOC) measurements, the soil samples were first treated with HCl (1M, 60 °C, 12 h) in order to remove carbonates, rinsed 5 times with Milli-Q water and dried (60 °C). Aliquots of around 50 µg were weighed into tin capsules for

BGD
10, 16903–16922, 2013

elemental and stable carbon isotopic analysis (FlashEA 1112 elemental analyzer (EA) coupled to a Thermo Scientific Delta V plus isotope ratio mass spectrometer (IRMS)).

For comparison with the compound-specific data, ^{14}C analysis was performed on bulk organic matter from the four Crvenka samples. Samples were first rinsed with 6 molar HCl at 60 °C for several hours to ensure complete removal of carbonates before rinsing (Milli-Q water) and drying (60 °C). Aliquots containing ~ 1 mg of carbon were weighed into tin boats and processed using automated graphitization equipment (AGE) 3 at the ETH Hönggerberg (Wacker et al., 2010b) prior to radiocarbon analysis.

2.3 Data processing

All compound-specific radiocarbon data were corrected for a vacuum line blank of 0.91 µg C with a fraction modern (Fm) of 0.23 ± 4.5 %. This value was determined in 2011 by analyses of 10 combined blanks, and is very similar to the vacuum line blank of Shah and Pearson (2007) who derived a blank value of 1 ± 0.2 µg C with a Fm of 0.2. Note that our blank assessment only accounts for contamination during the vacuum line process and is therefore lower than those reported for the entire laboratory process (Shah and Pearson, 2007; Ziolkowski and Druffel, 2009). All FAMEs were additionally corrected for the methyl group added during methylation. Bulk measurements were normalized and blank-subtracted against IAEA C3 cellulose and coal respectively. Radiocarbon ages were calculated using the Bats software (Wacker et al., 2010a) and converted to calendar ages using OxCal (Bronk Ramsey, 2009) and the Inc 09 calibration curve (Reimer et al., 2009). All ages in the text are calibrated.

3 Results

3.1 Leaf-wax concentrations in the soil profiles

Organic carbon- (C_{org}-) normalized concentrations of long-chain *n*-alkanes ($\sum nC_{25-35}$) and fatty acids ($\sum C_{24-34}$) show a sharp decrease with depth in both soil profiles in

BGD
10, 16903–16922, 2013

till (Fig. 2). This decrease is particularly pronounced in the Steinhof profile, where the uppermost sample was taken at a depth of only 10 cm, and leaf-wax concentrations are highest with ~ 20 µg (g C)$^{-1}$ for *n*-alkanes and ~ 6500 µg (g C)$^{-1}$ for fatty acids. The uppermost sample for the Niederbuchsiten profile was taken at a depth of 30 cm and therefore yields already relatively low concentrations. Below a depth of 40 cm concentrations of only 0.2–0.6 µg (g C)$^{-1}$ (*n*-alkanes) and 4–16 µg (g C)$^{-1}$ (fatty acids) were found in both profiles. The concentrations in most of these subsurface samples are below the limit of quantification (10 times blank) and some are even below the limit of detection (3 times blank).

These results suggest that either no or only very small quantities of long-chain *n*-alkanes and fatty acids are produced and accumulated at depth. Additional (i.e., post-sedimentary) sources of these compounds at depth, for example related to roots or microbial activity, are therefore unlikely to be significant.

3.2 Compound-specific radiocarbon analysis of leaf-wax biomarkers in loess

Concentrations of most *n*-alkane and fatty acid homologues were sufficient for radiocarbon analyses in the 4 samples from the LPS Crvenka. However, some compounds, (e.g., even C-numbered *n*-alkanes and odd C-numbered fatty acids) had to be combined prior to ^{14}C analysis. Results are summarized in Fig. 3 and documented in Table 1.

The Holocene soil sample Cr 1 exhibits ages between 1 and 2 ka BP. Only the even *n*-alkanes are significantly older (~ 4 ka BP). Radiocarbon ages of plant wax biomarkers from Cr 10 and Cr 20 are ~ 23 and ~ 28 ka BP, respectively, in good agreement with the chronostratigraphy. Sample Cr 40 has radiocarbon ages up to 45 ka BP and can therefore be regarded as almost carbon dead, which is consistent with its stratigraphic position. While the bulk age for Cr 20 is 26 ka BP and thus also reasonably consistent, the bulk age for Cr 10 is only 18.7 ka BP and thus significantly too young. This could be due to the presence of (acid-resistant) organic material derived from modern roots, as Cr 10 is only 2 m below the surface and roots are found at least down to that depth.

BGD
10, 16903–16922, 2013

Overall, however, the molecular-level ^{14}C measurements reveal that leaf-wax biomarkers are of similar age as the surrounding sediments, implying that post-sedimentary contributions by roots or microbes are negligible. Sample Cr 40, for example, has only ~ 1 % modern carbon (Table 1).

In more detail, the compound-specific radiocarbon ages reveal several interesting patterns. Cr 1, for example, is the only sample that shows much younger ages for the fatty acids than the alkanes. Cr 1 is also the only sample that has a much older age for the even *n*-alkanes than for the odd ones. And, finally, the nC_{25} and nC_{27} alkanes and C_{24} and C_{26} *n*-alkanoic acids are systematically younger than the corresponding longer homologues. We will come back to these three observations in the following discussion.

4 Discussion

4.1 Evaluating the contribution of fossil lipids

There are several lines of evidence that point to the absence of significant quantities of leaf-wax lipids derived from fossil sources. First, with respect to potential contributions of re-worked plant waxes, fossil *n*-alkanes are often characterized by low odd-over-even carbon number predominance (OEP), with OEP values close to 1 (e.g. Villanueva et al., 1997). OEP values for our samples are much higher (~ 10) indicative for largely unaltered vascular plant inputs. Likewise, even-over-odd predominance values of the fatty acids in these samples is ~ 4.

Second, a significant contribution of fossil, reworked lipids would lead to higher ages of the even *n*-alkanes compared to the odd homologues (and vice versa for the fatty acids). For instance, Pearson and Eglinton (2000) reported higher ages for the even *n*-alkanes and lower ages for the dominant odd *n*-alkanes in marine sediments. They explained this pattern with higher contributions of even *n*-alkanes from fossil (thermogenic) sources, because the latter have no odd-over-even predominance. With the

BGD
10, 16903–16922, 2013

exception of sample Cr 1, the samples from the LPS Crvenka do not show such an age pattern. Sample Cr 1 may contain some fossil alkanes related to recent human activities (Lichtfouse and Eglinton, 1995), but the difference in fraction modern carbon between even and odd compounds is small (0.6 vs. 0.75, Table 1).

Third, greater ^{14}C ages for *n*-alkanes than for fatty acids have been reported for marine sediments (Kusch et al., 2010; Pearson et al., 2001; Uchida et al., 2005). This has been interpreted to indicate the dominant terrestrial origin of, and fossil contributions to the *n*-alkanes, while fatty acids are more easily degraded during transport, and the relative importance of in situ production of some homologues by marine organisms may be higher. Apart from Cr 1, where a small age difference is observable, there are no significant differences between *n*-alkanes and fatty acids in the Crvenka samples. Consistent with the interpretation above, Cr 1 is the only sample which might contain non-negligible amounts of fossil *n*-alkanes.

Fourth, while variable $\delta^{13}C$ values among homologues could indicate inputs from more than one source (Liu et al., 2007), $\delta^{13}C$ values of individual compounds are relatively similar (~ −29 to −34 ‰), implying a narrow suite of source inputs.

It should be noted that the above arguments do not rule out synsedimentary contribution of leaf-waxes rapidly transported from remote dust source regions, because these signals could have comparable homologue patterns and radiocarbon ages as the leaf-waxes produced locally. Little is known about possible airborne transport of lipid biomarkers, and more research has to be conducted in order to assess this possibility in a more quantitative manner.

4.2 Evaluating post-sedimentary contributions

Although the compounds in each sample have similar ages, a tendency towards older ages can be observed with increasing chain length. In particular, the nC_{25} and nC_{27} alkanes and C_{24} and C_{26} *n*-alkanoic acids are systematically younger than the corresponding longer homologues. This finding is in good agreement with published compound-specific radiocarbon ages of fatty acids in soils (Matsumoto et al., 2007)

BGD
10, 16903–16922, 2013

and fluvially-dominated sediments (Drenzek et al., 2007). For soils, the pattern has been explained as a consequence of (i) better solubility of short chain fatty acids and therefore easier downward leaching into the subsurface and (ii) preferential degradation and production of shorter fatty acids by soil microorganisms. The age pattern of the *n*-alkanes could stem from the same mechanisms. Given the strongly hydrophobic nature of long-chain *n*-alkanes, the influence of microbial activity is likely more relevant than solubility. The production of *n*-alkanes during early litter degradation has been suggested also based on litterbag studies (Nguyen Tu et al., 2011; Zech et al., 2011a).

A post-sedimentary input of leaf-wax lipids by roots is less likely. Firstly, our data from the soil profiles in till have shown that there is no significant input and accumulation of *n*-alkanes and fatty acids below the topsoils, and the compound-specific radiocarbon ages for the LPS Crvenka are overall consistent with independent age control. Secondly, assuming that the composition of root-derived *n*-alkanes is similar to the composition of the leaves (Kuhn et al., 2010), roots would make *all* homologues too young, which we do not observe. Microorganisms, on the other hand, even although their metabolism is heterotrophic at depth, can readily explain incorporation of at least some modern carbon in the shorter homologues as they also feed on young percolating dissolved organic matter.

5 Conclusions

Both approaches adopted in this study to test the stratigraphic integrity of leaf-wax biomarkers yielded strong evidence of a co-eval origin with the stratigraphic horizon. On the one hand, concentrations of characteristic plant wax biomarkers (long-chain *n*-alkanes and fatty acids) were negligible below the topsoil in the two investigated soil profiles in till. On the other hand, compound-specific ^{14}C analysis of the same suites of compounds in the LPS Crvenka yielded ages consistent with independent age control for this sequence based on luminescence and chronostratigraphy. We therefore conclude that sub-surface production, input and accumulation of plant wax lipids related to

BGD
10, 16903–16922, 2013

root, microbial or other post-sedimentary processes is negligible at the studied sites. Detailed analysis of the ages of individual *n*-alkyl lipid homologues further indicates that reworking of fossil lipids is also relatively unimportant. The topsoil represents a possible exception and may be related to recent human activity. The slightly younger ages of the nC_{25} and nC_{27} alkanes and the C_{24} and C_{26} fatty acids than their longer-chain counterparts may reflect the influence of microbial reworking.

Overall, our results confirm the stratigraphic integrity of plant wax lipids in LPS and underline the potential of plant wax-based proxies for paleoenvironmental reconstructions. Leaf wax lipids might in fact be particularly useful for dating LPS back to at least ~ 30 ka, because in contrast to bulk soil organic material, they do not appear to be influenced by root-derived carbon inputs.

Acknowledgements. We thank D. Montluçon for help in the laboratory and the SNF for funding (SNF Ambizione PZ00P2_131670).

References

Bini, A., Buoncristiani, J.-F., Couterrand, S., Ellwanger, D., Felber, M., Florineth, D., Graf, H. R., Keller, O., Kelly, M., Schlüchter, C., and Schoeneich, P.: Die Schweiz während des letzteiszeitlichen Maximums (LGM) 1 : 500 000, Swisstopo, 3084 Wabern, 2009.

Bitterli, T., Jordi, H., Gerber, M., Gnaegi, C., and Graf, H. R.: Geologischen Atlas der Schweiz 1 : 25 000, Blatt 1108: Murgenthal, Swisstopo, 3084 Wabern, 2011.

Bronk Ramsey, C.: Bayesian analysis of radiocarbon dates, Radiocarbon, 51, 337–360, 2009.

Drenzek, N. J., Montluçon, D. B., Yunker, M. B., MacDonald, R. W., and Eglinton, T. I.: Constraints on the origin of sedimentary organic carbon in the Beaufort Sea from coupled molecular ^{13}C and ^{14}C measurements, Mar. Chem., 103, 146–162, 2007.

Eglinton, T. I. and Eglinton, G.: Molecular proxies for paleoclimatology, Earth Planet. Sc. Lett., 275, 1–16, 2008.

Eglinton, T. I., Eglinton, G., Dupont, L., Montlucon, D., Sholkovitz, E., and Reddy, C. M.: Composition, age, provenance of organic matter in NW African dust over the Atlantic Ocean, Geochem. Geophys. Geosy., 3, 1–27, doi:10.1029/2001GC000269, 2002.

BGD
10, 16903–16922, 2013

Gocke, M., Kuzyakov, Y., and Wiesenberg, G. L. B.: Rhizoliths in loess – evidence for post-sedimentary incorporation of root-derived organic matter in terrestrial sediments as assessed from molecular proxies, Org. Geochem., 41, 1198–1206, 2010.
Gocke, M., Kuzyakov, Y., and Wiesenberg, G.: Differentiation of plant derived organic matter in soil, loess and rhizoliths based on *n*-alkane molecular proxies, Biogeochemistry, 112, 23–40, doi:10.1007/s10533-011-9659-y, 2013.
Ivy-Ochs, S., Schäfer, J., Kubik, P. W., Synal, H. A., and Schlüchter, C.: Timing of deglaciation on the northern Alpine foreland (Switzerland), Eclogae Geol. Helv., 97, 47–55, 2004.
Kadereit, A., Kind, C.-J., and Wagner, G. A.: The chronological position of the Lohne Soil in the Nussloch loess section – re-evaluation for a European loess-marker horizon, Quaternary Sci. Rev., 59, 67–86, 2013.
Kuhn, T. K., Krull, E. S., Bowater, A., Grice, K., and Gleixner, G.: The occurrence of short chain *n*-alkanes with an even over odd predominance in higher plants and soils, Org. Geochem., 41, 88–95, 2010.
Kusch, S., Rethemeyer, J., Schefuss, E., and Mollenhauer, G.: Controls on the age of vascular plant biomarkers in Black Sea sediments, Geochim. Cosmochim. Ac., 74, 7031–7047, 2010.
Lichtfouse, E. and Eglinton, T. I.: ^{13}C and ^{14}C evidence of pollution of a soil by fossil fuel and reconstruction of the composition of the pollutant, Org. Geochem., 23, 969–973, 1995.
Liu, W., Yang, H., Ning, Y., and An, Z.: Contribution of inherent organic carbon to the bulk $\delta^{13}C$ signal in loess deposits from the arid western Chinese Loess Plateau, Org. Geochem., 38, 1571–1579, 2007.
Liu, W. and Huang, Y.: Compound specific D/H ratios and molecular distributions of higher plant leaf waxes as novel paleoenvironmental indicators in the Chinese Loess Plateau, Org. Geochem., 36, 851–860, 2005.
Marković, S. B., Bokhorst, M. P., Vandenberghe, J., McCoy, W. D., Oches, E. A., Hambach, U., Gaudenyi, T., Jovanovi, M., Zöller, L., Stevens, T., and Machalett, B.: Late Pleistocene loess-palaeosol sequences in the Vojvodina region, north Serbia, J. Quaternary Sci., 23, 73–84, 2008.
Matsumoto, K., Kawamura, K., Uchida, M., and Shibata, Y.: Radiocarbon content and stable carbon isotopic ratios of individual fatty acids in subsurface soil: implication for selective microbial degradation and modification of soil organic matter, Geochem. J., 41, 483–492, 2007.

BGD
10, 16903–16922, 2013

Nguyen Tu, T. T., Egasse, C., Zeller, B., Bardoux, G., Biron, P., Ponge, J.-F., David, B., and Derenne, S.: Early degradation of plant alkanes in soils: a litterbag experiment using 13C-labelled leaves, Soil Biol. Biochem., 43, 2222–2228, 2011.

Pearson, A. and Eglinton, T. I.: The origin of n-alkanes in Santa Monica Basin surface sediment: a model based on compound-specific ^{14}C and ^{13}C data, Org. Geochem., 31, 1103–1116, 2000.

Pearson, A., MeNichol, A. P., Benitez-Nielson, B. C., Hayes, J. M., and Eglinton, T. I.: Origins of lipid biomarkers in Santa Monica Basin surface sediment: a case study using compound-specific analyses, Geochim. Cosmochim. Ac., 65, 3123–3137, 2001.

Reimer, P. J., Baillie, M. G. L., Bard, E., Bayliss, A., Beck, J. W., Blackwell, P. G., Ramsey, C. B., Buck, C. E., Burr, G. S., Edwards, R. L., Friedrich, M., Grootes, P. M., Guilderson, T. P., Hajdas, I., Heaton, T. J., Hogg, A. G., Hughen, K. A., Kaiser, K. F., Kromer, B., McCormac, F. G., Manning, S. W., Reimer, R. W., Richards, D. A., Southon, J. R., Talamo, S., Turney, C. S. M., van der Plicht, J., and Weyhenmeyer, C. E.: IntCal09 and Marine09 radiocarbon age calibration curves, 0–50000 years cal BP, Radiocarbon, 51, 1111–1150, 2009.

Shah, S. R. and Pearson, A.: Ultra-microscale (5–25 µg C) analysis of individual lipids by ^{14}C AMS: assessment and correction for sample processing blanks, Radiocarbon, 49, 69–82, 2007.

Stevens, T., Markovic, S. B., Zech, M., Hambach, U., and Sümegi, P.: Dust deposition and climate in the Carpathian basin over an independently dated last glacial-interglacial cycle, Quaternary Sci. Rev., 30, 662–681, 2011.

Synal, H. A., Stocker, M., and Suter, M.: MICADAS: a new compact radiocarbon AMS system, Nucl. Instrum. Meth. B, 259, 7–13, 2007.

Uchida, M., Shibata, Y., Ohkushi, K. I., Yoneda, M., Kawamura, K., and Morita, M.: Age discrepancy between molecular biomarkers and calcareous foraminifera isolated from the same horizons of Northwest Pacific sediments, Chem. Geol., 218, 73–89, 2005.

Villanueva, J. I., Grimalt, J. O., Cortiljo, E., Vidal, L., and Labeyrie, L.: A biomarker approach to the organic matter deposited in the North Atlantic during the last climatic cycle, Geochim. Cosmochim. Ac., 61, 4633–4646, 1997.

Wacker, L., Christl, M., and Synal, H. A.: Bats: a new tool for AMS data reduction, Nucl. Instrum. Meth. B, 268, 976–979, 2010a.

Wacker, L., Nìmec, M., and Bourquin, J.: A revolutionary graphitisation system: Fully automated, compact and simple, Nucl. Instrum. Meth. B, 268, 931–934, 2010b.

BGD
10, 16903–16922, 2013

Wacker, L., Fahrni, S. M., Hajdas, I., Molnar, M., Synal, H.-A., Szidat, S., and Zhang, Y. L.: A versatile gas interface for routine radiocarbon analysis with a gas ion source, Nucl. Instrum. Meth. B, 294, 315–319, 2013.

Wiesenberg, G. L. B., Gocke, M., and Kuzyakov, Y.: Fast incorporation of rootderived lipids and FAs into soil – evidence from a short term multiple $^{14}CO_2$ pulse labelling experiment., Org. Geochem., 41, 1049–1055, 2010.

Xie, S., Wang, Z., Wang, H., Chen, F., and An, C.: The occurrence of a grassy vegetation over the Chinese loess plateau since the last interglacial: the molecular fossil record, Sci. China Ser. D, 45, 53–62, 2002.

Zech, M., Buggle, B., Leiber, K., Markovic, S., Glaser, B., Hambach, U., Huwe, B., Stevens, T., Sümegi, P., Wiesenberg, G., and Zöller, L.: Reconstructing Quaternary vegetation history in the Carpathian Basin, SE Europe, using *n*-alkane biomarkers as molecular fossils: problems and possible solutions, potential and limitations, Quaternary Sci. J., 58, 148–155, doi:10.3285/eg.58.2.03, 2009a.

Zech, M., Zech, R., Morrás, H., Moretti, L., Glaser, B., and Zech, W.: Late Quaternary environmental changes in Misiones, subtropical NE Argentina, deduced from multi-proxy geochemical analyses in a palaeosol-sediment sequence, Quaternary Int., 196, 121–136, 2009b.

Zech, M., Andreev, A., Zech, R., Mueller, S., Hambach, U., Frechen, M., and Zech, W.: Quaternary vegetation changes derived from a loess-like permafrost palaeosol sequence in northeast Siberia using alkane biomarker and pollen analyses, Boreas, 39, 540–550, doi:10.1111/j.1502-3885.2009.00132.x, 2010.

Zech, M., Pedentchouk, N., Buggle, B., Leiber, K., Kalbitz, K., Markovic, S. B., and Glaser, B.: Effect of leaf litter degradation and seasonality on D/H isotope ratios of *n*-alkane biomarkers, Geochim. Cosmochim. Ac., 75, 4917–4928, 2011a.

Zech, R., Huang, Y., Zech, M., Tarozo, R., and Zech, W.: High carbon sequestration in Siberian permafrost loess-paleosols during glacials, Clim. Past, 7, 501–509, doi:10.5194/cp-7-501-2011, 2011b.

Zech, R., Zech, M., Markoviæ, S., Hambach, U., and Huang, Y.: Humid glacials, arid interglacials? Critical thoughts on pedogenesis and paleoclimate based on multi-proxy analyses of the loess-paleosol sequence Crvenka, Northern Serbia, Palaeogeogr. Palaeocl., 387, 165–175, 2013.

BGD
10, 16903–16922, 2013

Zhang, Z., Zhao, M., Eglinton, G., Lu, H., and Huang, C.-Y.: Leaf wax lipids as paleovegetational and paleoenvironmental proxies for the Chinese Loess Plateau over the last 170 kyr, Quaternary Sci. Rev., 25, 575–594, 2006.

Ziolkowski, L. A. and Druffel, E. R. M.: Quantification of extraneous carbon during compound specific radiocarbon analysis of black Carbon, Anal. Chem., 81, 10156–10161, 2009.

BGD

10, 16903–16922, 2013

Table 1. Results of compound-specific radiocarbon measurements. All radiocarbon ages were converted to calendar ages using OxCal (Bronk Ramsey, 2009) and the Inc 09 calibration curve (Reimer et al., 2009).

Sample	Compound	µg C	F ^{14}C	Error	Calendar age	Error	δ^{13}C (‰)
Cr 1							
C_{24}	FAMEs	25.94	0.869	0.0129	1090	200	−29.1
C_{26}	FAMEs	20.66	0.846	0.0146	1250	280	−29.8
C_{28}	FAMEs	14.60	0.801	0.0179	1730	400	−33.0
C_{30}	FAMEs	21.37	0.785	0.0134	2010	290	−31.4
$C_{25,27,29,31}$	FAMEs	24.64	0.822	0.0131	1510	230	−29.5
nC_{25-27}	*n*-alkane	12.94	0.758	0.0187	2280	470	−31.0
nC_{29}	*n*-alkane	18.11	0.752	0.0150	2340	390	−33.9
nC_{33-35}	*n*-alkane	9.85	0.765	0.0230	2520	230	−31.7
$nC_{26,28,30,32,34}$	*n*-alkane	10.09	0.605	0.0190	4480	620	−32.1
Cr 10							
nC_{29}	*n*-alkane	12.82	0.0719	0.00517	25 400	1600	−34.9
nC_{31}	*n*-alkane	32.47	0.0787	0.00304	24 400	880	−33.1
nC_{33-35}	*n*-alkane	29.68	0.0963	0.00347	22 500	850	−32.6
$nC_{26,28,30,32,34}$	*n*-alkane	9.56	0.0973	0.00562	22 500	1100	−33.3
Cr 20							
$C_{26,28,30,32}$	FAMEs	31.88	0.0518	0.00285	29 500	880	−32.9
nC_{25-27}	*n*-alkane	10.33	0.0837	0.00514	23 800	1200	−33.3
nC_{29}	*n*-alkane	22.44	0.0540	0.00303	28 300	870	−33.0
nC_{31}	*n*-alkane	14.19	0.0641	0.00388	26 600	1300	−33.5
$nC_{26,28,30,32,34}$	*n*-alkane	8.84	0.053	0.00497	28 400	1800	−33.0
Cr 40							
C_{26}	FAMEs	17.87	0.0251	0.00317	34 100	2300	−32.9
C_{28}	FAMEs	23.92	0.0046	0.00242	46 500	3500	−32.8
C_{30}	FAMEs	33.48	0.0090	0.00229	43 200	4200	−33.3
C_{32}	FAMEs	15.32	0.0052	> 50 %	> 45 700	–	−34.8
$C_{25,27,29,31,33}$	FAMEs	27.60	0.0471	0.00235	46 800	3100	−34.4
nC_{25-27}	*n*-alkane	6.35	0.0196	0.00508	37 300	5000	−34.4
nC_{29}	*n*-alkane	13.30	0.0077	0.00294	45 200	4800	−34.8
nC_{31}	*n*-alkane	17.99	0.0245	0.00289	34 300	2200	−33.7
$nC_{26,28,30,32,34}$	*n*-alkane	7.36	0.0074	0.00414	44 600	5300	−34.1

BGD
10, 16903–16922, 2013

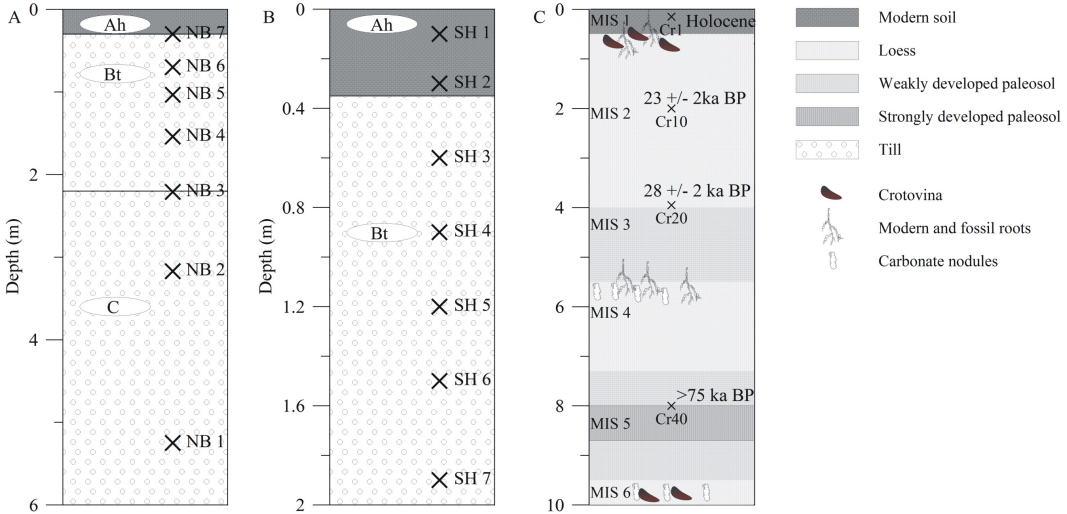

Fig. 1. Sketches of the soil profiles Niederbuchsiten **(A)** and Steinhof **(B)**, as well as the LPS Crvenka **(C)**. Samples selected for this study are marked, together with the estimated sediment ages.

BGD
10, 16903–16922, 2013

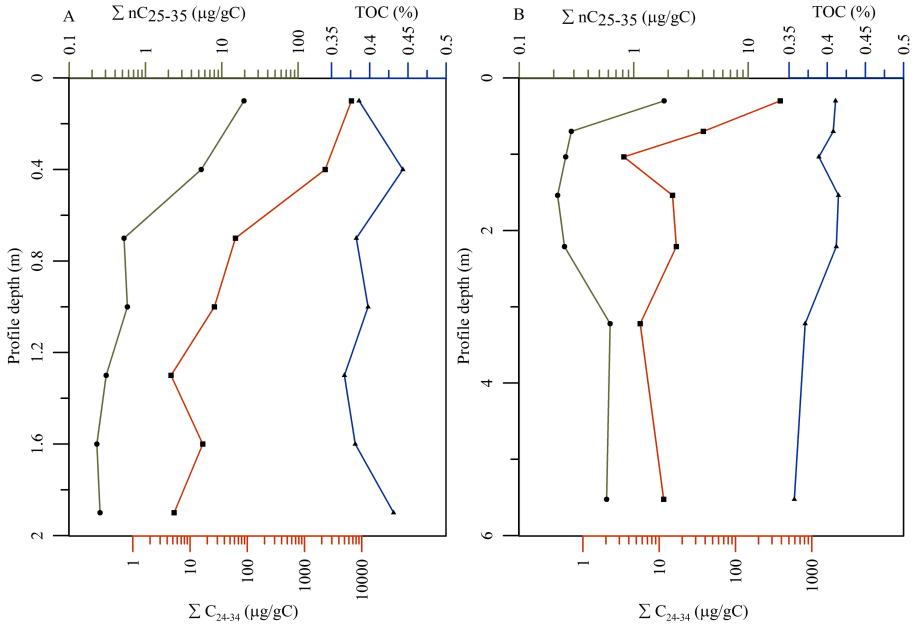

Fig. 2. TOC and leaf-wax concentrations in the soil profiles Steinhof **(A)** and Niederbuchsiten **(B)**. Note log concentration scale for $C_{25–35}$ *n*-alkanes and $C_{24–34}$ *n*-alkanoic acids.

BGD
10, 16903–16922, 2013

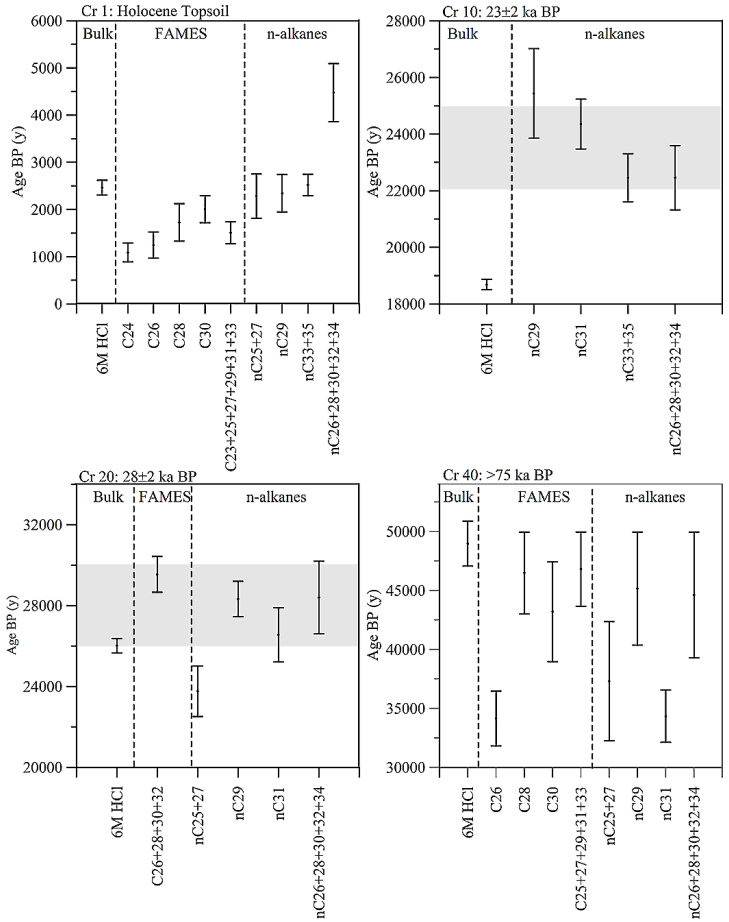

Fig. 3. Compound-specific and bulk radiocarbon ages (calibrated) for the four samples from the LPS Crvenka. The grey bars mark the sediment ages of Cr 10 (23 ± 2 ka BP) and Cr 20 (28 ± 2 ka BP) based on luminescence and stratigraphy.

BGD
10, 16903–16922, 2013